MICHIGAN STATE UNIVERSITY

CYCLOTRON LABORATORY

THERMAL PROPERTIES OF FINITE NUCLEAR SYSTEMS IN THE CONSTRAINED HARTREE-FOCK APPROXIMATION

H. SAGAWA and H. TOKI

OCTOBER 1984

MSUCL-489

MSUCL-489
October 1984

Thermal Properties of Finite Nuclear System in the Constrained Hartree-Fock Approximation

H. Sagawa

Cyclotron Laboratory, Michigan State University
East Lansing, MI 48824-1321, USA

and

H. Toki

Cyclotron Laboratory, Michigan State University
East Lansing, MI 48824-1321, USA

and

Department of Physics, Tokyo Metropolitan University
Setagaya, Tokyo 158, Japan

Abstract:

Saturation properties of thermal nuclei ^{90}Zr and ^{208}Pb are drastically changed at temperatures above T=6 MeV due to the fact that the minimum of the free energy becomes shallower. At T=6 MeV, the nuclear compression modulus is less than half of its value at T=0 MeV, and this decrease implies a very low excitation energy for the giant monopole state. The equation of state indicates the critical temperature of the liquid-gas phase transition at around $T_C \cong 10\text{-}15$ MeV, which occurs at very low density $\rho_C = 0.01\text{-}0.02$ fm^{-3}.

PACS numbers: 21.10.Dr, 21.10.Re, 21.60.Jz

Thermal properties of nuclei have been of great interest recently as a result of the data from intermediate-energy heavy-ion experiments.[1,2] The saturation properties of nuclear systems at finite temperatures are particularly interesting in relation to the giant compression mode[3] and the liquid-gas phase transition.[1,2,4] So far, these problems have been discussed in terms of nuclear matter calculation and the Thomas-Fermi approximation .

It is well-known that the saturation properties of nuclei are described very successfully over a wide range of mass at the zero temperature by the Hartree-Fock (H-F) approximation.[5] Recently, the H-F calculations at finite-temperature have been performed using two different interactions, namely, the Skyrme-type interaction[6] and the Bruckner G-matrix obtained by the Reid soft-core potential.[7] In order to study the phase-transition and the compression modulus of nucleus at finite-temperature, we must perform the constrained H-F calculation. Until now, such constrained H-F calculation for studying the diluted system has been done only at zero temperature.[8] In this work, we will discuss, for the first time, results of the constrained H-F calculations at several finite-temperatures. We have chosen medium and heavy nuclei ^{90}Zr and ^{208}Pb for this study.

The Hartree-Fock theory at finite-temperature might be formulated by the variation of the thermodynamical potential Ω,

$$\begin{aligned}\Omega &= \langle\hat{H}\rangle - T\cdot S - \mu\langle\hat{N}\rangle \\ &= \mathrm{Tr}\{\hat{H}D\} - T\cdot\mathrm{Tr}\{D\ \ell n\ D\} - \mu\ \mathrm{Tr}\{\hat{N}D\}\end{aligned} \tag{1}$$

with respect to the grand canonical partition function D of the system.[9] The expectation value for any operator is expressed by using the occupation

probability function of the single particle state $f_i(T)$. Thus, the entropy S is given by,

$$S = - \sum_i \{f_i(T)\ell n(f_i(T))+(1 - f_i(T))\ell n(1 - f_i(T))\} \quad (2)$$

The variation of the thermodynamical potential with respect to $f_i(T)$ gives the condition,

$$f_i(T) = 1/\{1 + \exp[(h_i - u)/T]\} \quad (3)$$

where $h_i(\rho)$ is the H-F hamiltonian density. Small changes of the trial wave functions around the fixed occupation probability leads to the equation,

$$h_i(\rho)\phi_i(T) = \varepsilon_i\phi_i(T) \quad (4)$$

This equation (4) should be solved self-consistently together with the subsidiary condition (3). In order to study the dilute system at finite temperature, we take a constrained-hamiltonian for the density,

$$h_i'(\rho) = h_i(\rho) - \lambda\rho(\vec{r}) \quad (5)$$

where the value λ is the Lagrange-multiplier.

We adopt a Skyrme-type density-dependent interaction SG II in the following calculations. The parameter set SG II has a lower power ($\rho^{1/6}$) of the density-dependence term and gives the compression modulus K_∞=218 MeV.[10] This interaction shows quite satisfactory results for the descriptions of the saturation properties of the ground state and the energy of the giant

resonances of many nuclei near the closed shells. We take 30 (40) single-particle states for proton and neutron configurations in the H-F calculations of ^{90}Zr (^{208}Pb). The H-F coupled equations (3) and (5) were solved by the Runge-Kutta method in the coordinate space with the maximum radius R=15 fm for ^{90}Zr and R=18 fm in ^{208}Pb.[11] As we will see later, these configuration spaces are not large enough to estimate properly the entropy at high-temperature above T=4 MeV. However, they seem to be sufficient to determine the H-F density and potential. Thus, we take into account the single-particle states until the N=15 major shell in the calculations of the entropy and the chemical potential. The single particle energies and wave functions above the lowest 30 states in ^{90}Zr (40 states in ^{208}Pb) are calculated in the fixed H-F potentials.

In Fig. 1, we plot the distributions of entropy and particle number with respect to the principle quantum number N in ^{208}Pb. These results are obtained with the unconstrained H-F equation (4). In the case of the low temperatures T=2 and 4 MeV, the dominant contribution to the entropy comes from the N=6 and 7 shells near the fermi surface. The entropy S is increasingly spread out among the higher shells when the temperature is increased. The summed contribution between the shell N=10 and N=15 is 29% of the total entropy at T=8 MeV and 35% at T=10 MeV. At the same time, for ^{208}Pb, the summed particle number above the N=10 shell which is zero at T=0 MeV goes up to 21.5 at T=8 MeV and 38 at T=10 MeV. We can see in the upper part of Fig. 1 that the entropy does not vanish even in the large space calculation including until the N=15 shell when the temperature is more than T=8 MeV. The contributions from the states above the N=15 shell are extrapolated by the smooth extension of the calculated lines until N=15 in

Fig. 1. The results in Fig. 2 and Table 1 include these contributions above N=15.

The saturation curves of the free energy $F=\langle\hat{H}\rangle-TS$ versus the root mean square (rms) radius for the mass distribution $r_m=\sqrt{\langle r^2\rangle_m}$ are drawn in Fig. 2 for ^{90}Zr and ^{208}Pb. Since our H-F results give the value r_m to be a smooth and unique function of the λ-value at each temperature, we can use the rms radius r_m instead of λ as a physical parameter for the study of the saturation properties in the following. We also summarize the various properties at the saturation point $(\partial(F/A)/\partial r_m=0)$ for different temperatures in Table 1. The binding energy and the rms radius for charge distribution at T=0 MeV are E/A=-8.74 MeV and r_C=4.27 fm for ^{90}Zr and E/A=-7.87 MeV and r_C=5.51 fm for ^{208}Pb. These can be compared with the experimental values E/A=-8.71 MeV and r_C=4.27 fm for ^{90}Zr and E/A=-7.87 MeV and r_C=5.50 fm for ^{208}Pb. The saturation point becomes shallower at the higher temperature, and the free energy F has no minimum above T=6 MeV in ^{90}Zr and above 7 MeV in ^{208}Pb. The rms radius values in Table 1 increase very slowly until T=4 MeV, but show sudden change at T=6 MeV both in ^{90}Zr and ^{208}Pb. The rapid change of the rms radius is also pointed out in the calculation of Ref. 9 for ^{208}Pb.

The compression modulus at each temperature can be defined by

$$K_A = r_m^2 \frac{\partial^2(F/A)}{\partial r_m^2} \tag{6}$$

at the saturation point. Due to the effect of the nuclear surface,[12] the value K_A of the finite system is 50% smaller than the nuclear matter value K_∞=218 MeV. We find that the temperature also decreases the K_A-value. The very low compression modulus and the large rms radius are both induced by

the reduction of the depth of the saturation minimum at high temperatures as is shown in Fig. 2.

The excitation energy of the giant monopole state can be related with the compression modulus by,[12]

$$\hbar\omega_{\lambda=0} = \sqrt{\hbar^2 K_A / m r_m^2} \tag{7}$$

with m being the nuclear mass. At zero temperature, this expression gives the energy $\hbar\omega_{\lambda=0}(T=0)=18.2$ MeV for ^{90}Zr and 14.1 MeV for ^{208}Pb, which are very close to the empirical values.[12] The rms radius r_m in Eq. (8) is increasing at high temperature, while the nuclear compression modulus is decreasing. These two changes cause a very rapid decrease in the excitation energy of the monopole state as is seen in Table 1. A similar feature is also found in a calculation of the quadrupole resonances by the RPA response function at finite temperature.[13] In terms of the momentum space, these results might be intimately related to the "melting" of the sharp fermi surface of the closed-shell nucleus. The extended Thomas-Fermi approximation[3] also shows the decrease of the K_A-value as a function of temperature, but the decrease is smaller than the present result.

In order to study the equation of state, we introduce the average density, related to the rms radius by $\bar{\rho}=3A/[4\pi(5r_m^2/3)^{3/2}]$. Defining the nuclear volume by $V=A/\bar{\rho}$, we can evaluate the pressure by the equation,

$$P = -\frac{\partial(F/A)}{\partial(V/A)} = \bar{\rho}^2 \frac{\partial(F/A)}{\partial\bar{\rho}} \tag{8}$$

The isothermal equation of states in ^{90}Zr and ^{208}Pb are shown in Fig. 3 until T=10 MeV. We plot the equation of state at very low density $\bar{\rho}\lesssim 0.01$

fm^{-3} as a smooth extension of the result until $\bar{\rho}\cong 0.01\ fm^{-3}$ and connected with the origin (P=0 and $\bar{\rho}=0$) of the figure.[14] At T=6 MeV, the average saturation density $\bar{\rho}(T=6)$ (corresponding to the pressure P=0 MeV.fm^{-3}) is half of the value $\bar{\rho}(T=0)$ in ^{208}Pb and one-quarter of $\bar{\rho}(T=0)$ in ^{90}Zr. On the other hand, in the nuclear matter calculation,[4] the saturation density changes only 10% in going from T=0 MeV to T=6 MeV. The magnitude of the pressure in the infinite system is generally much larger than the present result. This is due to the fact that the saturation minimum of nuclear matter is 2 times deeper in energy and the nuclear compression modulus is also 50% larger than the values for the finite system at T=0 MeV.

Concerning the critical temperature of the liquid-gas phase transition,[1,2,4] signaled as the disappearance of the local minimum in the P-$\bar{\rho}$ diagram, we are not able to provide a definite number due to the difficulties to solve the H-F equations at very low densities. However, the extrapolation of the available calculated results ^{90}Zr and ^{208}Pb indicate the critical temperature $T_C\cong 10-15$ MeV. Furthermore, the corresponding density would be around $\bar{\rho}_C\cong 0.01-0.02\ fm^{-3}$, which is far below that of infinite matter.

We would like thank to W.A. Friedman for careful reading of the manuscript. This work is supported by the National Science Foundation under grant no. PHY 83-12245.

References

1) M. W. Curtin et al, Phys. Lett. 123B, 289 (1983)

2) A. D. Panagiotou et al., Phys. Rev. Lett. 62, 405 (1984)

3) J. Meyer et al, Phys. Lett. 133B ,279 (1983)

4) G. Sauer et al, Nucl. Phys. A264, 221 (1976)

5) J. W. Negele, Rev. Mod. Phys. 54, 913 (1982)

6) P. Bonche et al, Nucl. Phys. A427, 278 (1984)

7) G. Bozzolo and J. P. Vary, Phys. Rev. Lett. 53, 903 (1984)

8) S. K. M. Wong et al, Nucl.Phys. A169, 294 (1971)

9) D. J. Thouless, The quantum mechanics of many-body systems (Academic Press, New York, 1972)

10) Nguyen van Giai and H. Sagawa, Phys. Lett. 106B, 379 (1981)

11) We should notice that the entropy and the rms radius above T=7 MeV are sensitive to the radius R. If we change the value R from 18 fm to 20 fm, the entropy and the rms radius are increased by 10~15% and 5~8%, respectively, above T=7 MeV. While the changes are less than 5% below T=6 MeV. The main features of the present results are not much affected by the change of the radius R. More precise calculation might be done by treating the liquid and vapor phases separately in the H-F calculation.[6]

12) J. Treiner et al, Nucl. Phys. A371, 253 (1982)

13) H. Sagawa and G. F. Bertsch, Phys. Lett. B, in press

14) Since the numerical accuracy becomes poor when the obtained rms radius is more than 10 fm due to the limit of the coordinate space by the radius R. Thus, we do not perform the H-F calculation below $\bar{\rho} \cong 0.01$ fm^{-3}.

Figure captions

Fig. 1 Entropy distribution ΔS (the upper part) and particle distribution ΔA (the lower part) with respect to the principle quantum number N of the shell model in ^{208}Pb at the Lagrange multiplier $\lambda=0$. The dotted lines of the upper figure are extracted from the numerical results until N=15.

Fig. 2 The free energies of ^{90}Zr and ^{208}Pb as a function on the rms radius r_m at various temperatures.

Fig. 3 The equation of state in ^{90}Zr and ^{208}Pb. The pressure is evaluated by Eq. (8). The dashed curve is drawn as an extrapolation of the curve until the density $\bar{\rho}\cong 0.01$ fm^{-3}. The dotted line shows the thermodynamical instability points for the single phase at each temperature. For details, see the text.

Table 1 Saturation properties of ^{90}Zr and ^{208}Pb. The entropy is obtained by Eq. (2), while the free energy and the thermal excitation energy are defined by $F=\langle\hat{H}\rangle - TS$ and $E^*=\langle\hat{H}\rangle_T - \langle\hat{H}\rangle_{T=0}$, respectively. For details, see the text.

	T(MeV)	S	F/A(MeV)	E^*(MeV)	μ_p(MeV)	μ_n(MeV)	r_m(fm)	K_A(MeV)	$\hbar\omega$(MeV)
	0.	0.	-8.74	0.	-5.74	-9.87	4.23	143.4	18.2
	2.	30.7	-9.03	34.9	-6.43	-10.07	4.27	121.0	16.6
^{90}Zr	4.	89.5	-10.53	156.7	-7.34	-11.30	4.87	58.5	10.1
	6.	211.4	-15.28	685.7	-9.74	-13.45	7.03	43.5	6.0
	0.	0.	-7.86	0.	-4.04	-6.17	5.52	147.	14.1
	2.	65.3	-8.09	81.3	-4.79	-7.39	5.60	121.	12.6
^{208}Pb	4.	152.4	-9.35	298.8	-5.50	-8.70	5.78	81.	10.0
	6.	313.2	-12.81	903.1	-7.15	-10.75	6.75	39.	5.9

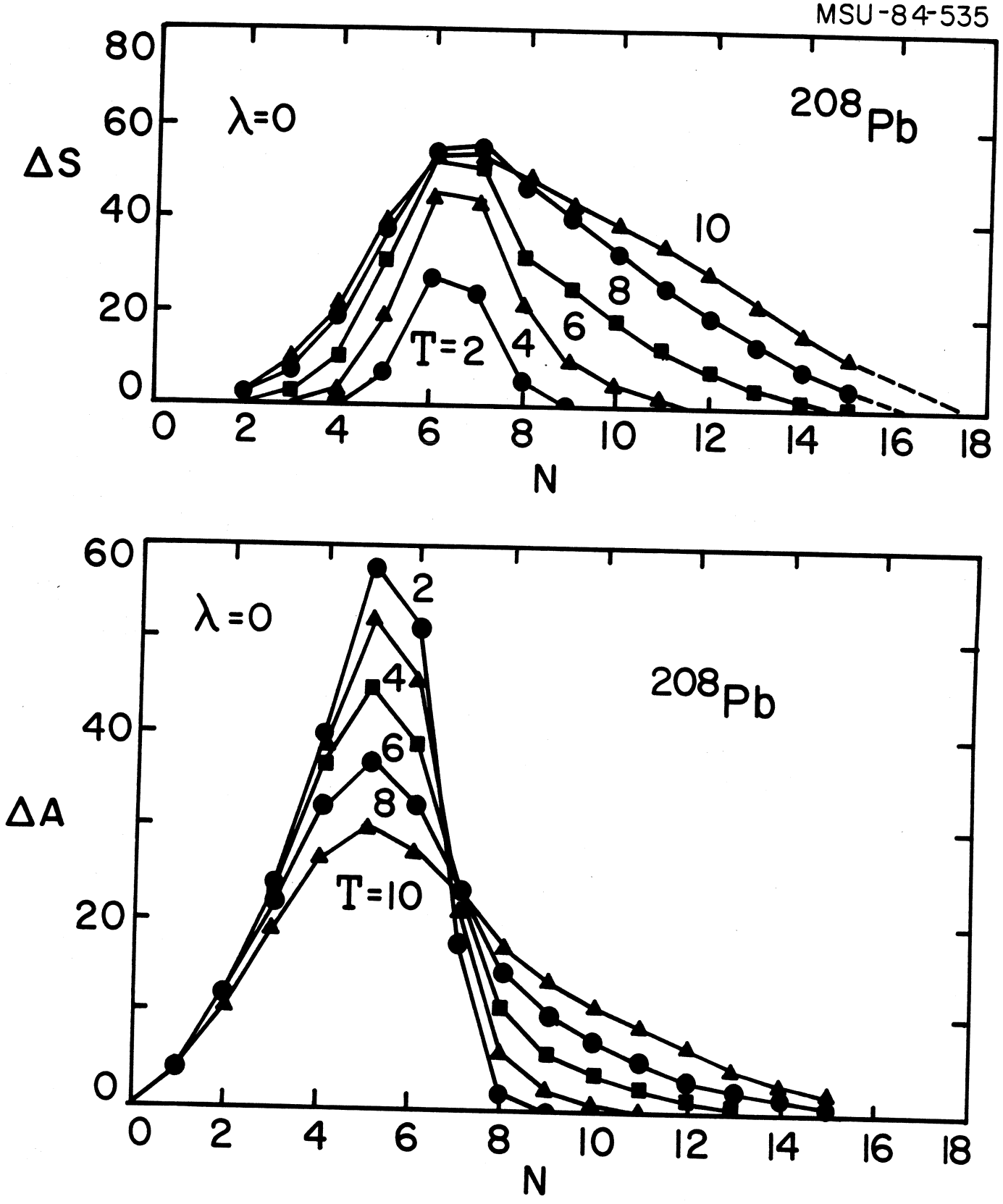

FIGURE 1

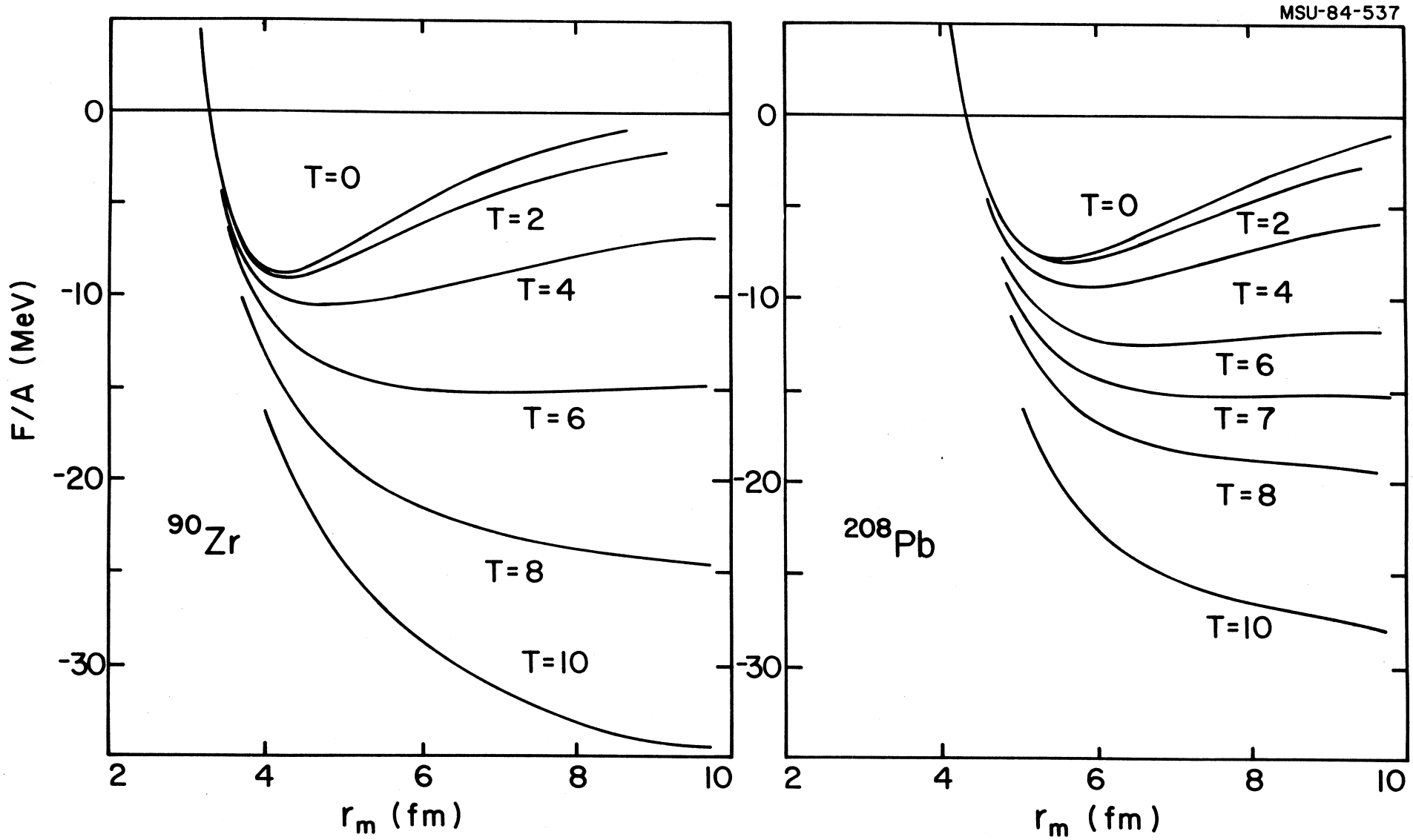
MSU-84-537
F/A (MeV)
0
-10
-20
-30
T=0
T=2
T=4
T=6
T=8
T=10
^{90}Zr
^{208}Pb
T=7
2
4
6
8
10
r_m (fm)

FIGURE 2

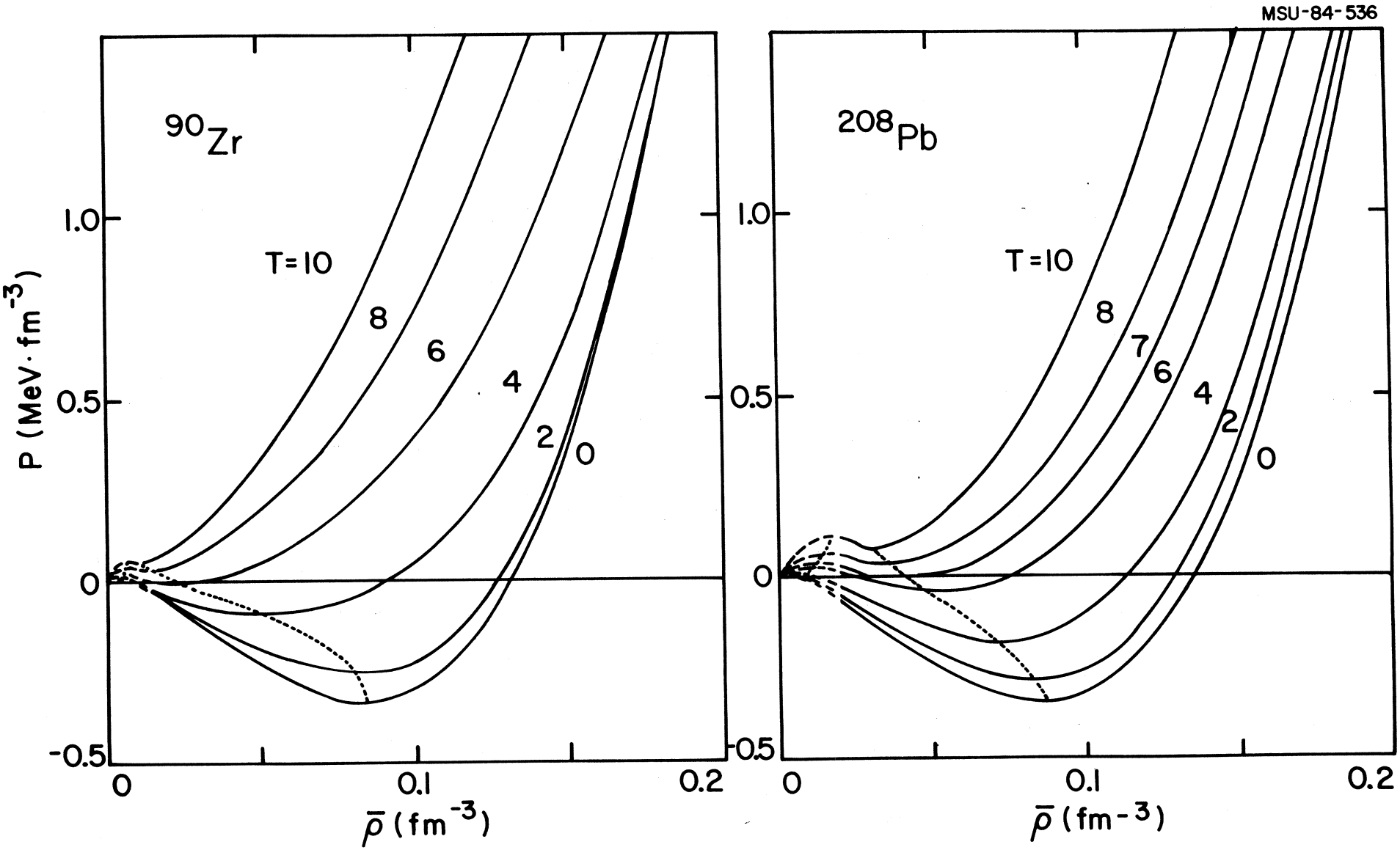
MSU-84-536
^{90}Zr
^{208}Pb
T=10
T=10
8
7
6
4
2
0
1.0
0.5
0
-0.5
0
0.1
0.2
P (MeV·fm^{-3})
$\bar{\rho}$ (fm^{-3})

FIGURE 3